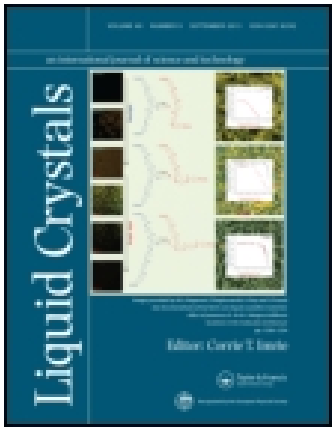

Liquid Crystals

Publication details, including instructions for authors and subscription information:
http://www.tandfonline.com/loi/tlct20

Anisotropic waveguide theory for electrically tunable distributed feedback laser from dye-doped holographic polymer dispersed liquid crystal

Zhihui Diao[ab], Wenbin Huang[ab], Zenghui Peng[a], Quanquan Mu[a], Yonggang Liu[a], Ji Ma[a] & Li Xuan[a]

[a] State Key Laboratory of Applied Optics, Changchun Institute of Optics, Fine Mechanics and Physics, Chinese Academy of Sciences, Changchun, Jilin, P.R. China

[b] University of Chinese Academy of Sciences, Beijing, P.R. China

Published online: 23 Oct 2013.

To cite this article: Zhihui Diao, Wenbin Huang, Zenghui Peng, Quanquan Mu, Yonggang Liu, Ji Ma & Li Xuan (2014) Anisotropic waveguide theory for electrically tunable distributed feedback laser from dye-doped holographic polymer dispersed liquid crystal, Liquid Crystals, 41:2, 239-246, DOI: 10.1080/02678292.2013.851289

To link to this article: http://dx.doi.org/10.1080/02678292.2013.851289

Liquid Crystals, 2014
Vol. 41, No. 2, 239–246, http://dx.doi.org/10.1080/02678292.2013.851289

Anisotropic waveguide theory for electrically tunable distributed feedback laser from dye-doped holographic polymer dispersed liquid crystal

Zhihui Diao[a,b], Wenbin Huang[a,b], Zenghui Peng[a], Quanquan Mu[a], Yonggang Liu[a], Ji Ma[a]* and Li Xuan[a]*

[a]*State Key Laboratory of Applied Optics, Changchun Institute of Optics, Fine Mechanics and Physics, Chinese Academy of Sciences, Changchun, Jilin, P.R. China;* [b]*University of Chinese Academy of Sciences, Beijing, P.R. China*

(*Received 30 August 2013; accepted 30 September 2013*)

Anisotropic waveguide theory is developed for electrically tunable distributed feedback (DFB) laser from dye-doped holographic polymer dispersed liquid crystal (HPDLC) grating. The period grating structure, optical anisotropy of the liquid crystal (LC) and practical light propagation path in the HPDLC have been considered. The emitted lasing wavelength is deduced on basis of the dielectric anisotropy of the LC, transverse-magnetic (TM) light wave propagation in the core layer and DFB laser theory. An experimental method to determine the tilt angle of the LC and the lasing behaviours under different electric fields are used to verify the validity of the anisotropic numerical analysis. The results show that a more accurate agreement between the theoretical calculations and the experimental data is achieved. The anisotropic numerical analysis presented here is very useful when designing and optimising tunable lasers for optical communications and integrated optics.

Keywords: holographic polymer dispersed liquid crystal; anisotropic waveguide; distributed feedback; electrically tunable laser

1. Introduction

Distributed feedback (DFB) waveguide lasers based on organic materials have attracted considerable attention recently because they are potentially used as compact components in optical communications and integrated optics [1–5]. Selective light amplification at specific wavelengths can be provided from the Bragg scattering in the DFB waveguide configuration. To be more functional and competitive, electrically tunable lasers were proposed by introducing liquid crystals (LCs) as active materials in the waveguide configurations [6–11]. As an efficient method to realise tunable lasers, holographic polymer dispersed liquid crystal (HPDLC) configuration has been developed. The HPDLC grating is fabricated by a mixture of LC and monomers exposed to two or multiple interfering laser beams. The monomers undergo a fast free-radical photopolymerisation in the bright regions of the interference pattern; counter-diffusions of the LC and monomers are initialised due to the resulting concentration gradient and alternating layers of the polymer in the bright fringes, and the LCs are formed in the dark fringes [12–24]. The formed periodic structure can be regarded as a one-dimensional photonic crystal that as optical resonator for emitted lasers [25,26]. Besides by electrical field, the HPDLC lasers can be tuned by other methods, such as thermal [27] and optical [28] effects. The former is caused by the decrease of the anisotropy of LC with the increase of temperature, and the latter is induced by the photoisomerisable dye changing the LC orientation under lights with different wavelengths.

The electrically tunable lasers based on dye-doped HPDLC grating have been reported before [26,29–32]. Although the experimental results are remarkable, no detailed theoretical or numerical analyses are given for electrically tunable dye-doped HPDLC lasers while the tunable lasing behaviours are only simply attributed to the reorientation of LC molecules upon the external electric field. In dye-doped HPDLC lasers, both polymer and LC should be considered because they are both in the light propagation path in the core layer. In our previous work, the electrically tunable transverse-magnetic (TM) mode laser was obtained, and the isotropic waveguide theory was adopted to explain the tunable lasing [32]. In that assumption, the different light modes would experience the same effective refractive index of the LC when propagating parallel with the cladding glass substrate. However, it cannot describe the practical situation since the different light modes will experience different refractive indices of the LC when they propagate in the different directions in the core layer, due to the LC optical anisotropy.

In this work, we take account of the LC optical anisotropic properties and develop anisotropic waveguide theory for dye-doped HPDLC laser. Previously such anisotropic analysis was only used to investigate the guide-mode composed by pure LC waveguides [33–35], while we introduce it to the DFB dye-doped

*Corresponding authors. Emails: jma2@kent.edu (Ji Ma); xuanli@ciomp.ac.cn (Li Xuan)

HPDLC laser system. The anisotropic waveguide theory is deduced and verified by the experiments of electrically tunable lasing behaviours and measurable reorientation degree of the LC in our HPDLC. The obtained anisotropic waveguide theory can be used to predict the lasing actions more precisely in different conditions such as the core layer thickness, LC birefringence and phase-separated LC amount.

2. Theory and experiment

2.1 *Anisotropic waveguide theory for HPDLC*

The HPDLC grating with polymer scaffolding morphology is mainly composed of polymer matrix and pure LC layer [23,36], as shown in Figure 1(a). In the polymer matrix, some trapped LC molecules are randomly aligned and not free to rotate by the external electric field [37]. In the pure LC layer, the LC alignment is parallel to the grating vector on average due to the polymer filaments. A parameter α is introduced to indicate the amount of the phase-separated LC, i.e., the ratio of pure LC layers in the whole grating. α can be obtained by birefringence measurement [23], and it is 19.16% in this work. A symmetric slab waveguide is consisted of the HPDLC configuration as the core and the two glass plates as the cladding substrates (Figure 1(b)). Here, the thickness of the indium-tin-oxide (ITO) layer is 30 nm, which is too thin to be considered in the waveguide structure [32].

When an electric field is applied, the LC molecules are rotated in x–z plane with a tilt angle θ, as shown in Figure 1(b). The refractive index of the LC experienced by the TM mode is different when the LC tilt angle is changed, and the TM mode laser can be tuned. On the other hand, the reorientation of the LC molecules has no influence on the transverse-electric (TE) mode since the TE mode always passes through the LC ordinary refractive index (n_o), no TE mode can be tuned. Taking TM_0 and TM_1 modes as examples (Figure 1 (b)), different TM mode lights propagate with different angles (θ_0 and θ_1) in the waveguide. When these modes pass through the pure LC layer, they will experience different refractive indices due to the LC optical anisotropy. We can see that in the core layer, the practical refractive index of TM mode in the LC layer is not only dependent on the Bragg condition but also on the LC tilt angle. Therefore, anisotropic waveguide theory needs to be developed for dye-doped HPDLC lasers to describe the true situation.

If the LC tilt angle θ is achievable, the relative permittivity of the pure LC layer can be expressed in a tensor form for optical anisotropy [34]:

$$\varepsilon_{LC} = \begin{bmatrix} \varepsilon_e \sin^2\theta + \varepsilon_o \cos^2\theta & 0 & \varepsilon_a \sin\theta\cos\theta \\ 0 & \varepsilon_o & 0 \\ \varepsilon_a \sin\theta\cos\theta & 0 & \varepsilon_e \cos^2\theta + \varepsilon_o \sin^2\theta \end{bmatrix}, \tag{1}$$

where $\varepsilon_a = \varepsilon_e - \varepsilon_o$, $\varepsilon_o = n_o^2$, $\varepsilon_e = n_e^2$, in which n_o and n_e are the ordinary and extraordinary LC refractive indices. Conversely, the polymer matrix with trapped LC is isotropic and constant, so its relative permittivity is given by:

$$\varepsilon_p = \left(\frac{2n_o^2 + n_e^2}{3}\right)\frac{1-\varphi_{pp}-\alpha}{1-\alpha} + n_{pp}^2\frac{\varphi_{pp}}{1-\alpha}, \tag{2}$$

where n_{pp} is the refractive index of the pure polymer and φ_{pp} is the volume proportion of the pure polymer in HPDLC grating. Therefore, the average relative permittivity of the HPDLC core layer ε_{core_layer} is:

$$\varepsilon_{core\_layer} = \begin{bmatrix} \varepsilon_{xx} & 0 & \varepsilon_{xz} \\ 0 & \varepsilon_{yy} & 0 \\ \varepsilon_{zx} & 0 & \varepsilon_{zz} \end{bmatrix} = (1-\alpha)\varepsilon_p + \alpha\varepsilon_{LC}. \tag{3}$$

Considering that the off-diagonal elements ε_{xz} and ε_{zx} are so small, compared with the diagonal ones, and there is no combination of TE and TM modes in our case, ε_{core_layer} can be simplified as:

$$\varepsilon_{core\_layer} = \begin{bmatrix} \varepsilon_{xx} & 0 & 0 \\ 0 & \varepsilon_{yy} & 0 \\ 0 & 0 & \varepsilon_{zz} \end{bmatrix}. \tag{4}$$

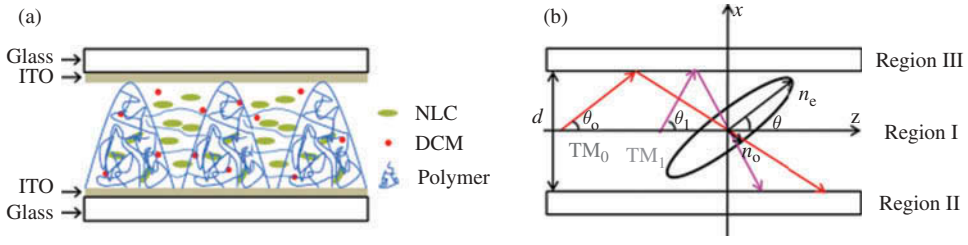

Figure 1. (colour online) (a) Schematic diagram of HPDLC grating and (b) propagation of TM mode lights in sample cell.

For the TM-polarised light wave ($\mathbf{H} = (0, H_y, 0)$, $\boldsymbol{E} = (E_x, 0, E_z)$) propagating in the HPDLC core layer along the z direction, its magnetic field can be expressed by:

$$\mathbf{H} = H_y(x)\exp[i(k_0 N z - \omega t)], \tag{5}$$

where k_0 and ω are the wave vector and angular frequency of the light, respectively, and N is the effective refractive index of TM mode. By substituting Equation (5) in the Maxwell's equation:

$$\nabla(\nabla \bullet \mathbf{H}) - \nabla^2\mathbf{H} = -\mu_0\varepsilon_0\varepsilon_{\text{core\_layer}}\frac{\partial^2\mathbf{H}}{\partial t^2}, \tag{6}$$

where μ_0 and ε_0 are the permeability and permittivity of vacuum, we will find the solution:

$$H_y(x) = \cos[k_0\sqrt{\frac{\varepsilon_{zz}}{\varepsilon_{xx}}(\varepsilon_{xx} - N^2)}x]. \tag{7}$$

Then, considering a symmetric waveguide composed of the anisotropic HPDLC as the core and the two isotropic glass plates with refractive index of n_g as substrates, the magnetic fields in these three regions can be expressed by [38]:

$$\begin{aligned}
H_{y\text{I}}(x) &= \cos\left[k_0\sqrt{\frac{\varepsilon_{zz}}{\varepsilon_{xx}}(\varepsilon_{xx} - N^2)}x + \phi\right] && \left(-\frac{d}{2} \le x \le \frac{d}{2}\right)\\
H_{y\text{II}}(x) &= \cos\left[-k_0\frac{d}{2}\sqrt{\frac{\varepsilon_{zz}}{\varepsilon_{xx}}(\varepsilon_{xx} - N^2)} + \phi\right]\exp\left[k_0\sqrt{N^2 - n_g^2}\left(x + \frac{d}{2}\right)\right] && \left(x < -\frac{d}{2}\right),\\
H_{y\text{III}}(x) &= \cos\left[k_0\frac{d}{2}\sqrt{\frac{\varepsilon_{zz}}{\varepsilon_{xx}}(\varepsilon_{xx} - N^2)} + \phi\right]\exp\left[k_0\sqrt{N^2 - n_g^2}\left(\frac{d}{2} - x\right)\right] && \left(x > \frac{d}{2}\right)
\end{aligned} \tag{8}$$

where d is the thickness of the core layer, Φ is a constant about phase and $H_{y\text{I}}$, $H_{y\text{II}}$ and $H_{y\text{III}}$ are the magnetic fields in the core layer ($-d/2 \le x \le d/2$), bottom glass substrate ($x < -d/2$) and upper glass substrate ($x > d/2$), respectively. According to the boundary conditions for transverse field components [39], we have:

$$\begin{aligned}
\frac{1}{\varepsilon_{zz}}\frac{\partial H_{y\text{I}}}{\partial x}\left(-\frac{d}{2}\right) &= \frac{1}{n_g^2}\frac{\partial H_{y\text{II}}}{\partial x}\left(-\frac{d}{2}\right)\\
\frac{1}{\varepsilon_{zz}}\frac{\partial H_{y\text{I}}}{\partial x}\left(\frac{d}{2}\right) &= \frac{1}{n_g^2}\frac{\partial H_{y\text{III}}}{\partial x}\left(\frac{d}{2}\right)
\end{aligned} \tag{9}$$

Thus an anisotropic waveguide equation for TM mode can be solved:

$$2\tan^{-1}\left[\frac{\varepsilon_{zz}}{n_g^2}\sqrt{\frac{\varepsilon_{xx}(N^2 - n_g^2)}{\varepsilon_{zz}(\varepsilon_{xx} - N^2)}}\right] + m\pi = k_0 d\sqrt{\frac{\varepsilon_{zz}}{\varepsilon_{xx}}(\varepsilon_{xx} - N^2)}, \tag{10}$$

where m is the mode number. Furthermore, according to the DFB laser theory [40], a TM mode in the waveguide will oscillate at a wavelength λ_{laser} so that its effective refractive index N obeys:

$$N = \frac{M\lambda_{\text{laser}}}{2\Lambda}, \tag{11}$$

where λ_{laser} is the emitted lasing wavelength, Λ is the grating period and M is the Bragg order. Combining Equations (4), (10) and (11), we have built a connection between the tilt angle θ and the lasing wavelength λ_{laser} and developed the anisotropic waveguide theory for dye-doped HPDLC laser.

2.2 *Experiment*

Two kinds of monomers were selected in our mixture. One was the dipentaerythritol hydroxyl pentaacrylate (DPHPA, Aldrich), and the other was the phthalic diglycol diacrylate (PDDA, Eastern Acrylic Chem). Photoinitiator Rose Bengal (RB, Aldrich) and coinitiator *N*-phenylglycine (NPG, Aldrich) were used to provide the sensitivity to green (532 nm) laser beam to form HPDLC grating. The LC TEB30A (Slichem, n_o = 1.522 and n_e = 1.692) and chain extender *N*-vinylpyrrolidinone (NVP, Aldrich) were also added. The laser dye 4-(dicyanomethylene)-2-methyl-6-(*p*-dimethylaminostyryl)-4H-pyran (DCM, Aldrich) was used as a gain medium for lasing action. These ingredients were mixed together with weight ratios of 27.3, 27.3, 0.5, 1.8, 33.0, 9.1 and 1.0 wt%, respectively, and then the pre-polymer syrup was injected into a sandwiched ITO glass cell by capillary action. A 532 nm Nd:YAG laser was used for the holographic recording. Two coherent s-polarised laser

beams were incident on one side of the sample cell with specific angle to create the transmission HPDLC grating. The grating pitch Λ is chosen at 804.8 nm, the cell thickness d is 2.5 μm and the refractive indices of the glass substrate n_g and pure polymer n_{pp} are 1.516 and 1.525, respectively.

The pump laser source for lasing action was a Q-switched 532 nm Nd:YAG pulsed laser with a pulse duration of 8 ns and repetition of 10 Hz. The laser beam was focused by a cylindrical lens on the sample to form a narrow strip gain area (7 mm long and 0.1 mm wide) along the grating vector to ensure sufficient DFB. In order to enable electrical modulation of the lasing wavelength, a square-wave voltage of 1 kHz frequency was applied on the sample. A polariser was placed before the fibre detector so that only TM mode laser can be collected from the edge of sample cell into a spectrometer (resolution: 0.25 nm). The detailed grating fabrication process and set-up for lasing measurement can be found elsewhere [23,24].

3. Results and discussion

3.1 LC reorientation upon electric field

A characterisation method, which was always applied to measure the pretilt angle of LC [41], is used here to determine the LC tilt angle under different electric fields, as shown in Figure 2. The HPDLC sample is mounted between a pair of mutually orthogonal polariser and analyser. A square-wave voltage is applied on the sample to reorientate the LC molecules. A probe light of 633 nm from He–Ne laser (744 μW) passes through the 45° polariser with respect to the y-axis and irradiates perpendicularly on the sample. The transmitted light will undergo a phase retardation caused by the LC existing in HPDLC grating and enter a photodetector.

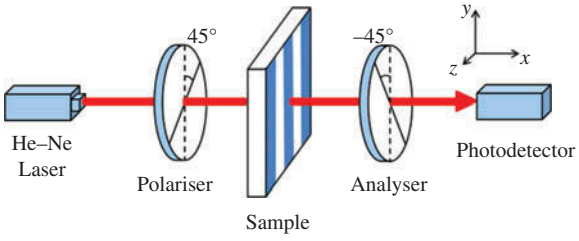

Figure 2. (colour online) Optical set-up to determine the tilt angle of LC.

The intensity of the transmitted light experienced a phase retardation caused by the birefringence effect of LC molecules in the pure LC layer [42] can be described by:

$$I_T = I_0 \sin^2\left[\frac{\pi d\alpha}{\lambda}\Delta n\right], \tag{12}$$

where λ and I_0 are the wavelength and intensity of the incident light, respectively, Δn is the birefringence of the LC molecules which varies with the LC tilt angle θ and it can be written as:

$$\Delta n = \frac{n_o n_e}{\sqrt{n_e^2 \sin^2\theta + n_o^2 \cos^2\theta}} - n_o. \tag{13}$$

From Equations (12) and (13), we can find that:

$$\frac{n_o n_e}{\sqrt{n_e^2 \sin^2\theta + n_o^2 \cos^2\theta}} = \frac{\lambda}{\pi d\alpha}\arcsin\sqrt{\frac{I_T}{I_0}} + n_o. \tag{14}$$

It can be seen that from Equation (14) that the tilt angle θ can be determined by measuring the intensity I_T and I_0 experimentally under arbitrary electric field.

The transmitted light was measured under different electric fields, as shown in Figure 3(a). It can be found that the intensity of the transmitted light

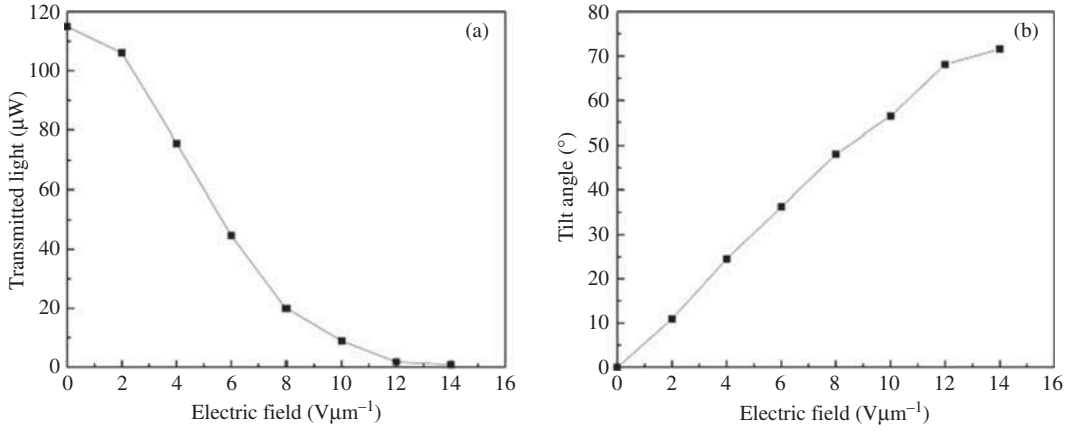

Figure 3. (a) Transmitted light and (b) LC tilt angle under different electric fields.

decreases with the increasing electric field, which means that the birefringence effect of the sample is weakened when the LC molecules tend to align their long axes to the field direction. According to Equation (14), the tilt angle was calculated and shown in Figure 3(b). As expected, the higher the electric field, the larger the tilt angle. Due to the thin cell gap that the sample could not bear the higher electric field, we did not drive the LC molecules to the saturation situation (90°). Upon the electric field of 14.0 $V\mu m^{-1}$, the tilt angle can reach 71.6° in our measurement. We will use the measured LC tilt angle to verify our anisotropic waveguide theory.

3.2 *Electrically tunable lasing behaviours*

Figure 4(a) shows the emission spectra of the dye-doped HPDLC laser under different electric fields. Multi-wavelength DFB lasing behaviours were observed from the sample. In the absence of the electric field, the lasing wavelengths were located at 615.4 nm and 612.6 nm for TM_0 and TM_1 modes, respectively. When the electric field exceeded the threshold 2.0 $V\mu m^{-1}$, the lasing wavelengths started to be tuned at the Freedericksz transition of the LC molecules. Above the electric field of 4.0 $V\mu m^{-1}$, TM_2 mode appeared at 610.6 nm. The maximum red-shift of lasing wavelengths was observed at 14.0 $V\mu m^{-1}$, whereas the higher electric field will exceed the bearing capability of our HPDLC sample with 2.5 μm cell gap. The relationship between the lasing wavelengths and the electric fields is summarised in Figure 4(b). As the electric field is increased, all TM modes are tuned to the longer wavelengths, and the spectral tuning of TM_0, TM_1 and TM_2 modes are 12.0 nm, 10.6 nm and 5.9 nm, respectively. Compared to the 8.0 nm reported in our previous work [32], the wider electrically tuning range is attributed to the higher phase-separation degree of LC (current 19.16% to previous 11.0%), since bigger grating period is chosen in this work. However, the bigger grating period needs a higher Bragg order to activate the lasing action according to Equation (11), which will result in a higher threshold energy and lower conversion efficiency [43,44].

3.3 *Lasing behaviours and anisotropic waveguide theory*

According to the LC tilt angle measured in Section 3.1, we summarised the experimental and calculated lasing wavelengths of the TM modes based on Equations (4), (10) and (11) in Table 1. From Table 1, we can find that a good agreement between the experimental data and theoretical calculations for all the TM modes, verifying the validity of the anisotropic waveguide theory for electrically tunable dye-doped HPDLC laser. However, due to the lower efficiency of the confinement for the higher-order mode in waveguide [43,44], we did not detect the TM_3 mode experimentally at 610.1 nm predicted by the theory.

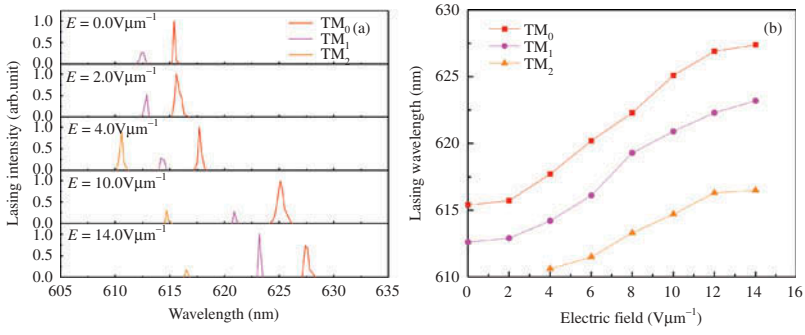

Figure 4. (colour online) (a) Emission spectra of the dye-doped HPDLC laser under different electric fields and (b) the relationship between the lasing wavelengths and electric fields.

Table 1. Experimental and theoretical lasing wavelengths under different electric fields[a].

		TM_0 (nm)		TM_1 (nm)		TM_2 (nm)		TM_3 (nm)	
Electric field ($V\mu m^{-1}$)	Tilt angle (°)	λ_{laser}	λ^*_{laser}	λ_{laser}	λ^*_{laser}	λ_{laser}	λ^*_{laser}	λ_{laser}	λ^*_{laser}
0	0	615.4	**615.5**	612.6	**612.6**	–	–	–	–
4	24.6	617.7	**617.8**	614.2	**614.5**	610.6	**610.2**	–	–
10	56.5	625.1	**624.6**	620.9	**620.5**	614.7	**614.7**	–	–
14	71.6	627.4	**627.4**	623.2	**622.8**	616.5	**616.9**	–	**610.1**

Note: [a]λ_{laser} is the experimental data, and λ^*_{laser} is the theoretical calculation.

Furthermore, we perform the comparison between the anisotropic waveguide theory proposed in this work and isotropic waveguide theory used in our previous work [32], for dye-doped HPDLC laser in Figure 5. It can be found that, although the difference between the blue solid line (anisotropic) and red dashed line (isotropic) is small, more experimental data show the trends in accordance with anisotropic waveguide theory. It indicates that the anisotropic waveguide theory is more accurate to describe the lasing behaviours of dye-doped HPDLC laser.

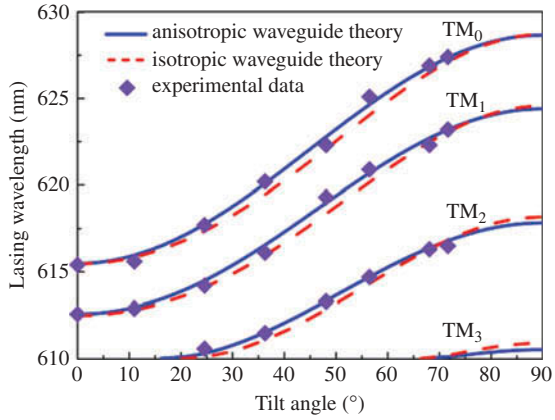

Figure 5. (colour online) Comparison between the anisotropic waveguide theory (blue solid line) and isotropic waveguide theory (red dashed line).

3.4 *Predicable lasing action by anisotropic waveguide theory*

More meaningfully, the anisotropic waveguide theory we develop here for dye-doped HPDLC laser would be very useful to design tunable lasers, predict and optimise their electro-tunable properties. For example, in this system, many factors can be considered to improve the tunable lasing action, such as the core layer thickness (d), LC birefringence (Δn) and phase-separated LC amount (α). If the grating period, LC birefringence and phase-separation degree of the LC are fixed same with our experiment, the tunable lasing action with different core layer thickness can be predicted, as shown in Figure 6(a) and 6(b). From this prediction, we can design and achieve a single-mode electrically tunable laser when the core layer thickness is smaller than 0.75 μm. If the core layer thickness is fixed and different LC with bigger birefringence such as 0.25 or 0.35 [45] is used to optimise the TM_0 lasing action, a higher Δn can lead to a wider tunable lasing range, as shown in Figure 6(c), in which the maximum shift of lasing wavelength can reach 29 nm when designing Δn is 0.35 and n_o is 1.522. If the phase-separation degree is optimised, it can be found

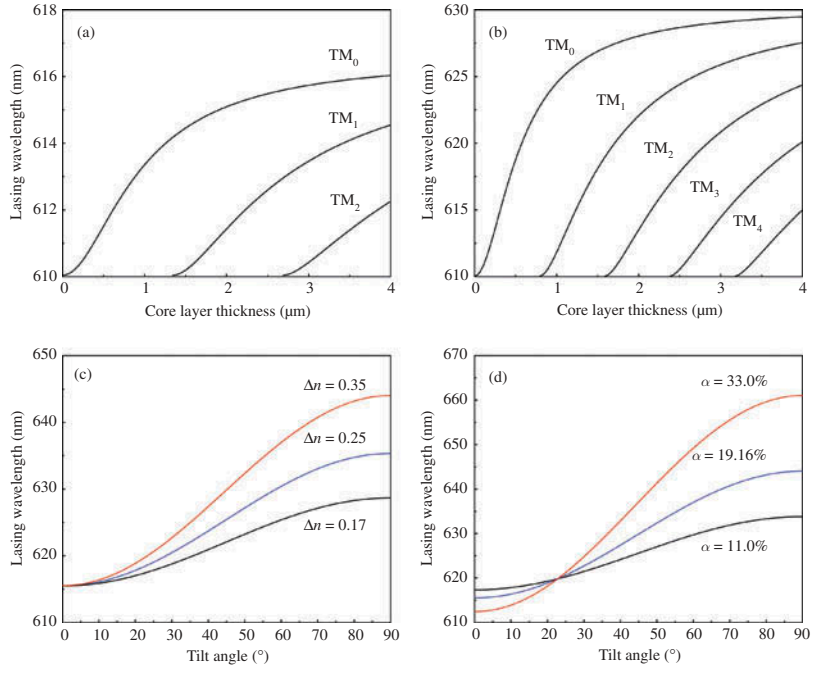

Figure 6. (colour online) Predicable lasing action according to the anisotropic waveguide theory: (a) with LC tilt angle 0° and (b) 90° (simulation parameters: Λ = 804.8 nm, n_o = 1.522, Δn = 0.17 and α = 19.16 %); (c) with 0.17, 0.25, 0.35 LC birefringence (simulation parameters: Λ = 804.8 nm, d = 2.5 μm, n_o = 1.522 and α = 19.16 %); and (d) phase-separation degree of LC (simulation parameters: Λ = 804.8 nm, d = 2.5 μm, n_o = 1.522 and Δn = 0.35).

that not only the tunable lasing range but also the initial lasing wavelength position without applying the electric field can be designed and optimised, as shown in Figure 6(d). These three examples further show that the anisotropic waveguide theory can be utilised to design, predict and optimise the tunable lasing behaviours for optical communications and integrated optics. The optimal work of electrically tunable DFB dye-doped HPDLC laser based on our anisotropic analysis is undergoing.

4. Conclusions

In conclusion, the anisotropic waveguide theory has been developed for electrically tunable DFB dye-doped HPDLC laser based on the lasing properties and LC optical anisotropic properties. The LC tilt angle is obtained experimentally to verify the validity of the anisotropic waveguide theory. The results show that the better agreement between the anisotropic theoretical calculations and experimental data is achieved, which provide more accurate numerical analysis to describe the electrically tunable lasing behaviours, compared with isotropic analysis. Moreover, this accurate anisotropic analysis will predict the lasing action when designing or optimising the tunable lasers for practical applications.

Funding

This work is supported by the National Natural Science Foundation of China [grant numbers 11174274, 11174279, 61205021 and 11204299].

References

[1] Duarte FJ. Tunable laser applications. 2nd ed. New York (NY): CRC Press; 2009.
[2] Dragoman D, Dragoman M. Advanced optoelectronic devices. New York (NY): Springer; 1998.
[3] Coles H, Morris S. Liquid-crystal lasers. Nat Photon. 2010;4:676–685.
[4] Clark J, Lanzani G. Organic photonics for communications. Nat Photon. 2010;4:438–446.
[5] Orignac X, Barbier D, Du XM, Almeida RM. Fabrication and characterization of sol-gel planar waveguides doped with rare-earth ions. Appl Phys Lett. 1996;69:895–897.
[6] Ozaki M, Kasano M, Kitasho T, Ganzke D, Haase W, Yoshino K. Electro-tunable liquid-crystal laser. Adv Mater. 2003;15:974–977.
[7] Ozaki R, Shinpo T, Yoshino K, Ozaki M, Moritake H. Tunable liquid crystal laser using distributed feedback cavity fabricated by nanoimprint lithography. Appl Phys Express. 2008;1:012003.
[8] Ozaki R, Matsuhisa Y, Ozaki M, Yoshino K. Electrically tunable lasing based on defect mode in one-dimensional photonic crystal with conducting polymer and liquid crystal defect layer. Appl Phys Lett. 2004;84:1844–1846.
[9] Maune B, Loncar M, Witzens J, Hochberg M, Baehr-Jones T, Psaltis D, Scherer A, Qiu YM. Liquid-crystal electric tuning of a photonic crystal laser. Appl Phys Lett. 2004;85:360–362.
[10] Yu HP, Tang BY, Li JH, Li L. Electrically tunable lasers made from electro-optically active photonics band gap materials. Opt Express. 2005;13:7243–7249.
[11] Matsui T, Ozaki M, Yoshino K. Electro-tunable laser action in a dye-doped nematic liquid crystal waveguide under holographic excitation. Appl Phys Lett. 2003;83:422–424.
[12] Yang DK, Wu ST. Fundamentals of liquid crystal devices. New York (NY): John Wiley & Sons Inc; 2006.
[13] Sutherland RL, Natarajan LV, Tondiglia VP, Bunning TJ, Adams WW. Electrically switchable volume gratings in polymer-dispersed liquid crystals. Appl Phys Lett. 1994;64:1074–1076.
[14] Bunning TJ, Natarajan LV, Tondiglia VP, Sutherland RL. Holographic polymer-dispersed liquid crystals (H-PDLCs). Annu Rev Mater Sci. 2000;30:83–115.
[15] White TJ, Natarajan LV, Tondiglia VP, Bunning TJ, Guymon CA. Polymerization kinetics and monomer functionality effects in thiolene polymer dispersed liquid crystals. Macromolecules. 2007;40:1112–1120.
[16] De Sio L, Caputo R, De Luca A, Veltri A, Umeton C, Sukhov AV. In situ optical control and stabilization of the curing process of holographic gratings with a nematic film-polymer-slice sequence structure. Appl Opt. 2006;45:3721–3727.
[17] Caputo R, De Sio L, Veltri A, Umeton C, Sukhov AV. Development of a new kind of switchable holographic grating made of liquid-crystal films separated by slices of polymeric material. Opt Lett. 2004;29:1261–1263.
[18] Liu YJ, Su YC, Hsu YJ, Hsiao VK. Light-induced spectral shifting generated from azo-dye doped holographic 2D gratings. J Mater Chem. 2012;22:14191–14195.
[19] Zheng Z, Song J, Liu Y, Guo F, Ma J, Xuan L. Single-step exposure for two-dimensional electrically-tunable diffraction grating based on polymer dispersed liquid crystal. Liq Cryst. 2008;35:489–499.
[20] Zheng Z, Ma J, Liu Y, Xuan L. Molecular dynamics of the interfacial properties of partially fluorinated polymer dispersed liquid crystal gratings. J Phys D Appl Phys. 2008;41:235302.
[21] Huang W, Deng S, Li W, Peng Z, Liu Y, Hu L, Xuan L. A polarization-independent and low scattering transmission grating for a distributed feedback cavity based on holographic polymer dispersed liquid crystal. J Opt. 2011;13:085501.
[22] Huang W, Diao Z, Liu Y, Peng Z, Yang C, Ma J, Xuan L. Distributed feedback polymer laser with an external feedback structure fabricated by holographic polymerization technique. Org Electron. 2012;13:2307–2311.
[23] Huang W, Liu Y, Diao Z, Yang C, Yao L, Ma J, Xuan L. Theory and characteristics of holographic polymer dispersed liquid crystal transmission grating with scaffolding morphology. Appl Opt. 2012;51:4013–4020.
[24] Diao Z, Deng S, Huang W, Xuan L, Hu L, Liu Y, Ma J. Organic dual-wavelength distributed feedback laser

empowered by dye-doped holography. J Mater Chem. 2012;22:23331–23334.
[25] Liu YJ, Sun XW, Shum P, Li HP, Mi J, Ji W, Zhang XH. Low-threshold and narrow-linewidth lasing from dye-doped holographic polymer-dispersed liquid crystal transmission gratings. Appl Phys Lett. 2006;88:061107.
[26] Hsiao VKS, Lu CG, He GS, Pan M, Cartwright AN, Prasad PN, Jakubiak R, Vaia RA, Bunning TJ. High contrast switching of distributed-feedback lasing in dye-doped H-PDLC transmission grating structures. Opt Express. 2005;13:3787–3794.
[27] Luo D, Sun XW, Dai HT, Demir HV, Yang HZ, Ji W. Temperature effect on the lasing from a dye-doped two-dimensional hexagonal photonic crystal made of holographic polymer-dispersed liquid crystals. J Appl Phys. 2010;108:013106.
[28] Tong HP, Li YR, Lin JD, Lee CR. All-optically controllable distributed feedback laser in a dye-doped holographic polymer-dispersed liquid crystal grating with a photoisomerizable dye. Opt Express. 2010;18:2613–2620.
[29] Jakubiak R, Bunning TJ, Vaia RA, Natarajan LV, Tondiglia VP. Electrically switchable, one-dimensional polymeric resonators from holographic photopolymerization: a new approach for active photonic bandgap materials. Adv Mater. 2003;15:241–244.
[30] Jakubiak R, Tondiglia VP, Natarajan LV, Sutherland RL, Lloyd P, Bunning TJ, Vaia RA. Dynamic lasing from all-organic two-dimensional photonic crystals. Adv Mater. 2005;17:2807–2811.
[31] Jakubiak R, Natarajan LV, Tondiglia V, He GS, Prasad PN, Bunning TJ, Vaia RA. Electrically switchable lasing from pyrromethene 597 embedded holographic-polymer dispersed liquid crystals. Appl Phys Lett. 2004;85:6095–6097.
[32] Huang W, Diao Z, Yao L, Cao Z, Liu Y, Ma J, Xuan L. Electrically tunable distributed feedback laser emission from scaffolding morphologic holographic polymer dispersed liquid crystal grating. Appl Phys Express. 2013;6:022702.
[33] Asquini R, Fratalocchi A, d'Alessandro A, Assanto G. Electro-optic routing in a nematic liquid-crystal waveguide. Appl Opt. 2005;44:4136–4143.
[34] Abbate G, De Stefano L, Santamato E. Transverse-magnetic nonlinear modes in a nematic liquid-crystal slab waveguide. J Opt Soc Am B. 1996;13:1536–1541.
[35] Lin TS, Lue JT. Mode splitting in an optical slab waveguide filled with nematic liquid crystals. Appl Phys B-Lasers O. 2003;76:561–567.
[36] Vardanyan KK, Qi J, Eakin JN, De Sarkar M, Crawford GP. Polymer scaffolding model for holographic polymer-dispersed liquid crystals. Appl Phys Lett. 2002;81:4736–4738.
[37] Butler JJ, Malcuit MS, Rodriguez MA. Diffractive properties of highly birefringent volume gratings: investigation. J Opt Soc Am B. 2002;19:183–189.
[38] Yamamoto S, Koyamada Y, Makimoto T. Normal-mode analysis of anisotropic and gyrotropic thin-film waveguides for integrated optics. J Appl Phys. 1972;43:5090–5097.
[39] Okamoto K. Fundamentals of optical waveguides. 2nd ed. San Diego (CA): Academic Press; 2010.
[40] Kogelnik H, Shank CV. Stimulated emission in a periodic structure. Appl Phys Lett. 1971;18:152–154.
[41] Chen KH, Chang WY, Chen JH. Measurement of the pretilt angle and the cell gap of nematic liquid crystal cells by heterodyne interferometry. Opt Express. 2009;17:14143–14149.
[42] Amosova LP, Vasil'ev VN, Ivanova NL, Konshina EA. Ways of increasing the response rate of electrically controlled optical devices based on nematic liquid crystals. J Opt Technol. 2010;77:79–87.
[43] Matsui T, Ozaki M, Yoshino K. Tunable laser action in a dye-doped nematic liquid-crystal waveguide under holographic excitation based on electric-field-induced TM guided-mode modulation. J Opt Soc Am B. 2004;21:1651–1658.
[44] Tsutsumi N, Nishida H. Tunable distributed feedback lasing with low threshold and high slope efficiency from electroluminescent conjugated polymer waveguide. Opt Commun. 2011;284:3365–3368.
[45] Peng Z, Liu Y, Cao Z, Mu Q, Yao L, Hu L, Yang C, Wu R, Xuan L. Fast response property of low-viscosity difluorooxymethylene-bridged liquid crystals. Liq Cryst. 2013;40:91–96.